SCIENTIFIC OASIS

Spectrum of Mechanical Engineering and Operational Research

Journal homepage: www.smeor-journal.org
eISSN: 3042-0288


# Liver Tissue Surrogates: Development and Biomechanical Characterization

Gurpreet Singh[1], Arnab Chanda[1,2*]

[1] Centre for Biomedical Engineering, Indian Institute of Technology Delhi, New Delhi, India
[2] Department of Biomedical Engineering, All India Institute of Medical Sciences Delhi, India

**ARTICLE INFO**

***Article history:***
Received 23 March 2024
Received in revised form 11 July 2024
Accepted 22 July 2024
Available online 30 July 2024

***Keywords:***
Artificial Tissue; Liver; Surrogates; Biomechanical Testing; Hyperelastic.

**ABSTRACT**

Human liver tissue often suffers extensive damage during impact-based trauma injuries, such as those that happen in vehicle accidents. However, it is challenging to study the biomechanics of human liver tissue under different loading situations through experiments in a clinical context due to ethical and biosafety concerns. In this work, biofidelic liver tissue surrogates, which exhibit realistic mechanical characteristics, have been developed for the first time. The tissue surrogates were made using a four-part elastomer material that could be cast to any size or form, mimicking the mechanical behavior of the liver tissue. The tissue's behavior was tested under six different strain rates, ranging from low to high, and its non-linear mechanical behavior was characterized using the Yeoh hyperelastic curve fit model. To the best of our knowledge, no liver tissue surrogates have been developed which possess the same biomechanical properties as real liver tissue. The use of precisely developed tissue simulants can be beneficial for surgical training, trauma research, and the development of medical models for different liver disorders such as liver cirrhosis, fatty liver, and liver fibrosis.

## 1. Introduction

Damage to the abdominal organs has been a pioneering topic of study in the field of biomedical engineering. This is because automobile accidents can cause tension and compression impact loads, which can lead to severe damage to the abdominal organs. The liver tissue, the second largest organ in the abdominal cavity after the skin, is often affected in such accidents [1,2]. As one of the visceral organs in the human body, the liver is responsible for various functions, including the storage of minerals and vitamins, the absorption of bile into the small intestine, and many other vital functions. Therefore, it is important to determine the strength of the liver tissue under a wide range of compressive and tensile loading circumstances, which can help biomedical engineers to better understand the mechanical characteristics of the liver tissue and develop effective treatments for liver damage caused by accidents and explosions [3].

* *Corresponding author.*
*E-mail address: Arnab.chanda@cbme.iitd.ac.in*

https://doi.org/10.31181/smeor11202412

There are two types of collagen, I and III, found in the liver [4]. When subjected to shear or tensile loading, these collagen fibers show great mechanical strength. Therefore, it's important to understand the tasks they perform in the liver tissue when it's under strain [5]. When the liver tissue is under stress, it's crucial to know whether the load is aligned with the fiber orientation. If the load is in the same direction as the collagen fibers, the tensile strength of the tissue will be higher than against the orientation of the fibers. This is because the fibers move in the same direction. The mechanical characteristics of liver tissue have not yet been fully understood. Researchers have used different approaches to determine the in vivo mechanical properties of human liver tissue under single-axis loading, such as aspiration tests and optical approaches [6]. They have also used transient elastography and dynamic mechanical analysis to determine the elastic modulus of porcine and human liver tissues [7,8]. Sakuma *et al.*, [9] calculated the stress-strain diagrams of pig liver tissue when it was subjected to tensile and compressive loadings. The mechanical characteristics of liver tissue have been studied using animal models such as pig and bovine [10,11]. Stingl *et al.,* [12] conducted the first research to test human liver tissue, which was undertaken a few decades ago. Recently, Karimi *et al.,* [13] evaluated fresh cadaveric samples to determine the mechanical characteristics of human liver tissue for a wide range of objectives, such as research on trauma, diagnostics, surgical planning, damage biomechanics, and more [14].

Experimental tests on liver tissue in a clinical setting to determine its mechanical properties are difficult due to ethical and biosafety concerns. Moreover, the mechanical properties of the liver tissue vary significantly due to tissue dehydration that occurs after death, which increases with the time elapsed since death [15]. To overcome these challenges, an elastomer-based material system was used to simulate the mechanical properties of liver tissue. The fabricated liver tissue surrogates are easy to use, can be cast into any desired geometry, and do not raise any ethical or biosafety issues. The non-linear behavior of the liver tissue surrogates was analyzed using the Yeoh hyperelastic curve fit model. These precisely developed liver tissue surrogates with realistic mechanical characteristics can be used for a wide range of applications, including liver biomechanics, trauma research, surgical planning, and diagnostic purposes. Section 2 covers the fabrication of sample coupons for potential liver tissue surrogates, mechanical testing of the generated samples, and hyperelastic material modeling for liver tissue surrogates. Section 3 presents the results and discussion of the pioneering work, followed by conclusions, limitations, and future scope of the reported work in Section 4.

## 2. Methodology

### *2.1 3D Printed Mold for the Fabrication of Sample Coupons*

SolidWorks (Dassault Systèmes, Vélizy-Villacoublay, France) was used to design a mold with the dimensions of 15cm × 11cm × 0.5cm for fabricating test coupon samples. The mold was 3D printed using polylactic acid (PLA) on a Voxelab Aquila printer manufactured by Zhejiang Flashforge 3D Technology Co., Ltd. in China. The mold was designed to produce 15 coupons, each measuring 5cm in length, 1cm in width, and 0.3cm in thickness. A four-part elastomer-based material was poured into the mold and cured for five to six hours. Figure 1 shows both the 3D mold and the test coupons made using the four-part elastomers for the tests.

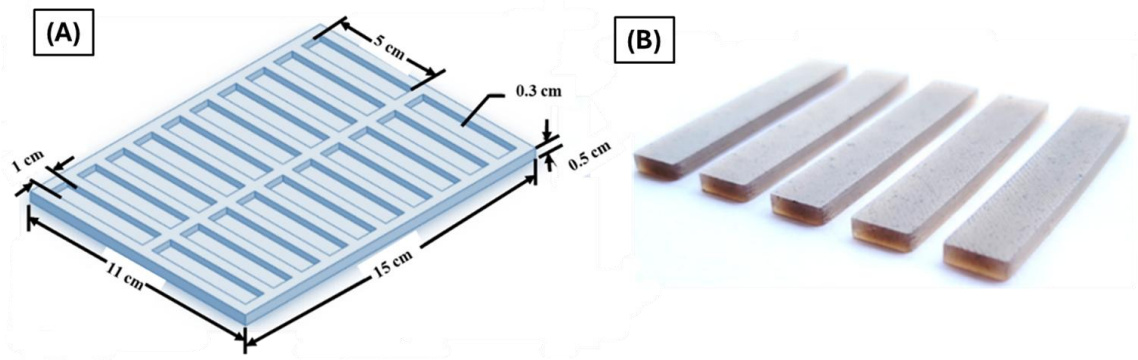


**Fig. 1.** Schematic of the designed mold for fabricating sample coupons in (A) and fabricated test coupons in (B)

*2.2 Candidate Test Coupon Samples for the Liver Tissue Surrogates*

The candidate test coupons for liver tissue surrogates were fabricated using a four-part elastomer-based material system. The elastomer material of different shore hardness, namely shore 5A, 15A, and 30A, was supplied by Chemzest Enterprises in Chennai, India. To ensure the material's hardness complied with the American Society for Testing and Materials (ATSM) D2240 standards, the shore durometer was used to check it [16]. To fabricate sample coupons with different shore hardness ranging from 5A to 15A, the two-part elastomer with shore 5A was mixed with the two-part elastomer with shore 15A in the specified ratios to make a four-part elastomer solution. The same process was used to create sample coupons with shore hardness ranging from 16A to 30A, using the four-part elastomer with shore 15A (two-part) and shore 30A (two-part). The four-part mixture was weighed, mixed homogeneously, and poured into the 3D mold for curing. The material compositions used in the fabrication of the sample coupons for the experimental trials conducted to determine liver tissue surrogates are included in Table 1. To make it easier to refer to the different parts, part A and part B of the 5A shore hardness material were referred to as 1A and 1B, respectively. Similarly, parts A and B of the 15A shore hardness were referred to as 2A and 2B, while parts A and B of 30A were referred to as 3A and 3B.

**Table 1**
Material composition for fabricating the sample coupons (by wt. %)

| Sample coupon for uniaxial testing | Composition of the elastomer material | Shore hardness of sample coupon |
|---|---|---|
| Test 1 | 50%1A-50%1B | 5A |
| Test 2 | 45%1A-45%1B-5%2A-5%2B | 6A |
| Test 3 | 35%1A-35%1B-15%2A-15%2B | 8A |
| Test 4 | 25%1A-25%1B-25%2A-25%2B | 10A |
| Test 5 | 15%1A-15%1B-35%2A-35%2B | 12A |
| Test 6 | 5%1A-5%1B-45%2A-45%2B | 14A |
| Test 7 | 50%2A-50%2B | 15A |
| Test 8 | 47%2A-47%2B-3%3A-3%3B | 16A |
| Test 9 | 40%2A-40%2B-10%3A-10%3B | 18A |
| Test 10 | 33%2A-33%2B-17%3A-17%3B | 20A |
| Test 11 | 27%2A-27%2B-23%3A-23%3B | 22A |
| Test 12 | 20%2A-20%2B-30%3A-30%3B | 24A |
| Test 13 | 13%2A-13%2B-37%3A-37%3B | 26A |
| Test 14 | 7%2A-7%2B-43%3A-43%3B | 28A |
| Test 15 | 50%3A-50%3B | 30A |

*1A and 1B represent the two-part elastomer of shore 5A*

*2A and 2B represent the two-part elastomer of shore 15A*
*3A and 3B represent the two-part elastomer of shore 30A*

### *2.3 Mechanical Testing of the Candidate Liver Tissue Surrogates*

In order to record the force versus displacement data of each sample, a universal testing machine was used to test the test coupon samples for liver tissue surrogates. When conducting uniaxial tensile testing on soft materials, a few things need to be considered [15,17,18]. Firstly, specific grips are required to prevent the sample from sliding around while the test is being performed. Secondly, the difference in strain rates substantially impacts the stress versus strain responses of the soft materials being tested mechanically. These materials have to be assessed at a certain strain rate to evaluate the results from testing human tissues. Thirdly, the response values of the tensile test may also be affected by the dimensional geometry of the test sample [19]. Each of these aspects was taken into consideration in the current work, and the experimental trials were conducted accordingly. During the studies, the potential test coupon samples for the surrogates were carefully held, and specified sample dimensions were determined to prevent slippage.

For each specimen, six different strain rates were applied: 0.16mm/sec, 0.4mm/sec, 0.5mm/sec, 0.8mm/sec, 1mm/sec, and 2.5mm/sec. All of the 15 samples were tested at each of these strain rates, resulting in a total of 90 tests (15 samples × 6 strain rates). The range of strain rates was selected based on previous studies where these were used to investigate the mechanical characteristics of different cadaveric tissue samples [13,20–26]. The chosen range had a minimum strain rate of 0.16mm/s and a maximum strain rate of 2.5mm/s. Before each trial, an initial load of 0.1N was applied to ensure that there was no slack in the system. To ensure the accuracy and reproducibility of the results, each sample was tested three times at each strain rate simultaneously. After the sample was clamped in the UTM grips, it had dimensions of 30mm × 10mm × 3mm, which matched the dimensions reported in previous research [27,28]. To create an engineering stress-engineering strain plot, the force-displacement data obtained during each experimental test was converted. Several stages were involved in processing the force-displacement data. First, negative force-displacement values were removed from the curves. Second, the graphs were shifted to the origin, and negative load values present at the beginning of the tensile test due to positive displacements were excluded from consideration. The initial slack of the sample material may have caused both these values to be insignificant for the analysis of results. Figure 2 shows the experimental setup for the uniaxial testing of liver tissue surrogate test coupons.

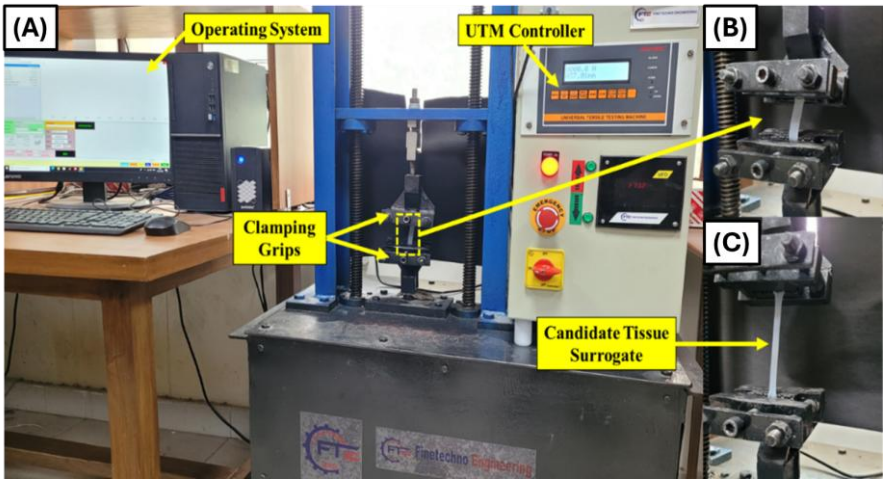


**Fig. 2.** (A) Tensile testing setup for the candidate liver tissue surrogates, (B) Sample coupon before the test, and (C) after the test

### *2.4 Hyperelastic Material Modeling for the Liver Tissue Surrogates*

Human soft tissues, as well as materials based on elastomers, exhibit non-linear mechanical behavior [29]. In this study, liver tissue surrogates were developed, and their non-linear behavior was described using the Yeoh hyperelastic curve fit model. The Yeoh hyperelastic material model is a model for the deformation of nearly incompressible, nonlinear elastic materials such as elastomers. It is a 3rd-order reduced polynomial model that exhibited a good convenience to fit the Test Data curve. The Yeoh model was also used to estimate the non-linear properties of several soft tissues, including tongue and tonsils tissue, stomach tissue, brain tissue, etc. [28,30,31]. It is important to note that hyperelastic material models depend on the strain energy function, known as '$\Psi$', and the type of material [17]. Moreover, any hyperelastic model is dependent on either the invariants of Cauchy-Green tensors *($I_1$, $I_2$,* and *$I_3$)* or on the primary stresses *($\lambda_1$, $\lambda_2$, $\lambda_3$)*, as seen in Eq. 1-4. Eq. 5 shows the strain energy function *($\Psi$)* of the hyperelastic curve fit model used in this investigation.

$$\psi = \psi(I_1, I_2, I_3) \tag{1}$$

$$I_1 = \sum_{i=1}^{3} \lambda_i^2 \tag{2}$$

$$I_2 = \sum_{i,j=1}^{3} \lambda_i^2 \lambda_j^2,\ i \neq j \tag{3}$$

$$I_3 = \prod_{i=1}^{3} \lambda_i^2 \tag{4}$$

$$\psi_{Yeoh} = \sum_{i=1}^{3} c_i\,(I_1 - 3)^i \tag{5}$$

Eq. 6 expresses the primary Cauchy stress using the stretch energy function and the strain energy function. To calculate and curve-fit the non-linear stress versus strain behavior of a uniaxially tested sample, Eq. 7 can be used [32]. This involves making use of Eq. 5 for the strain energy function of the Yeoh hyperelastic model and Eq. 6 for the primary Cauchy stress.

$$\sigma_1 = \lambda_1 \frac{\partial \psi}{\partial \lambda_1} - \lambda_3 \frac{\partial \psi}{\partial \lambda_3},\ \sigma_2 = \sigma_3 = 0 \tag{6}$$

$$\sigma_{Yeoh} = 2\left(\lambda^2 - \frac{1}{\lambda}\right)(c_1 + 2c_2(I_1 - 3) + 3c_3(I_1 - 3)^2) \tag{7}$$

In Section 3, we discussed the results obtained from the Yeoh hyperelastic curve fit model for liver tissue surrogates. To evaluate the accuracy of the chosen curve fit model in predicting the non-linear behavior of the liver tissue surrogates, we used the $R^2$ correlation approach. The $R^2$ value ranges from 0 to 1, where 0 indicates the least satisfactory fit, and 1 indicates the most satisfactory match. Previous research literature suggested that liver tissue behaves either isotropically or transversely isotropically under uniaxial testing and tensile loading conditions [32–34]. Therefore, our assumption of isotropic material behavior for liver tissue surrogates is reasonable.

## 3. Results and Discussion

### *3.1 Mechanical Behavior of the Liver Tissue Surrogates*

To fabricate the test coupons for the liver tissue surrogates, the elastomer material's composition was mixed to develop a range of samples (as detailed in section 2). The samples were then subjected to uniaxial testing to evaluate their mechanical properties. Figure 3 shows the stress versus strain plots for all the trials, along with the stress versus strain range of the human liver tissue, as reported in the literature [13]. The stress versus strain curves were plotted using the mean stress values of each test coupon (i.e., test 1 to test 15). Error bars were added to represent the range of stresses observed across all the strain rates.

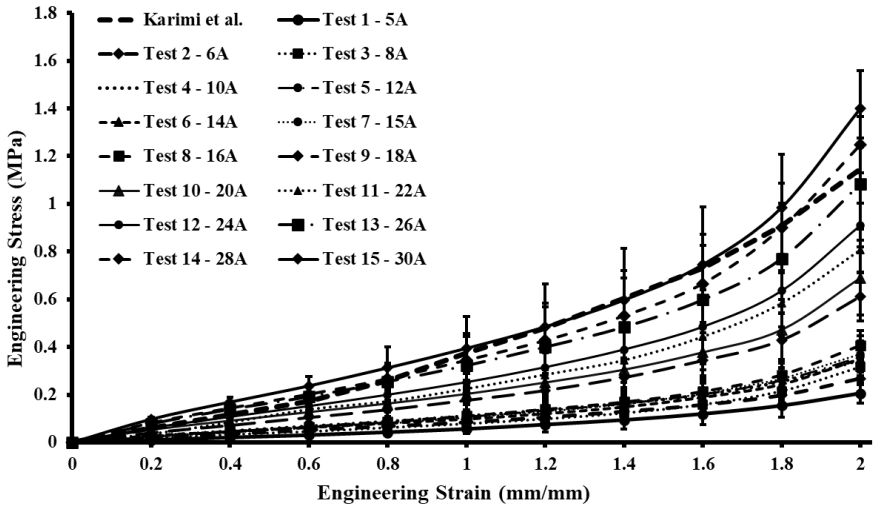


**Fig. 3.** Comparison of stress versus strain plot of the candidate liver tissue surrogates with the literature [13]

*3.2 Repeatability Test with Controlled Samples*

Fourteen out of the fifteen test coupon samples, liver tissue surrogates showed significant results, except for test 15. The stress-strain curves of these test coupons were consistent with the literature on cadaveric human liver tissue [13], and they were able to imitate the mechanical properties of human tissue, as shown in Figure 4. The stress values calculated for each of the six strain rates, as the average plus or minus the standard deviation, were either lower or very close to the literature limit [13].

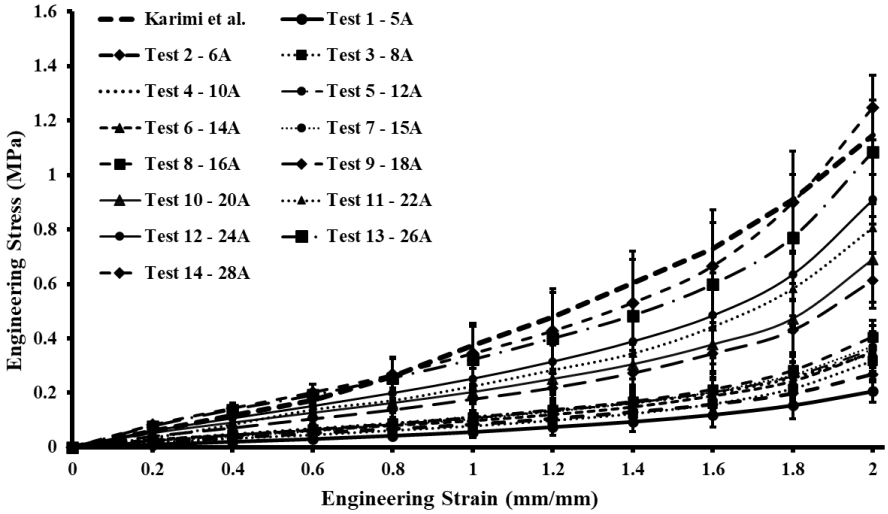


**Fig. 4.** Stress versus strain plot of the tested samples mimicking the mechanical behavior of liver tissue [13]

At low strain rates (0.16mm/s, 0.4mm/s, and 0.5mm/s), the predicted stress values were below the literature limit, while at high strain rates (0.8mm/s, 1mm/s, and 2.5mm/s), they exceeded the literature bound [13]. The sample with shore hardness 28A (i.e., test 14) closely resembled the mechanical characteristics of liver tissue and was selected as the controlled liver tissue surrogate for the repeatability test. Three specific samples of the controlled specimen were fabricated for the repeatability test, and five different sets of tests were conducted to confirm the findings. Figure 5 displays the mean values of the results, the error bars of the five sets for the repeatability test, and

the literature limit for liver tissue [13]. The controlled sample (i.e., test 14) was not labeled to limit the findings but to perform a comparative analysis with the experimental results on the cadaveric liver tissue from the literature.

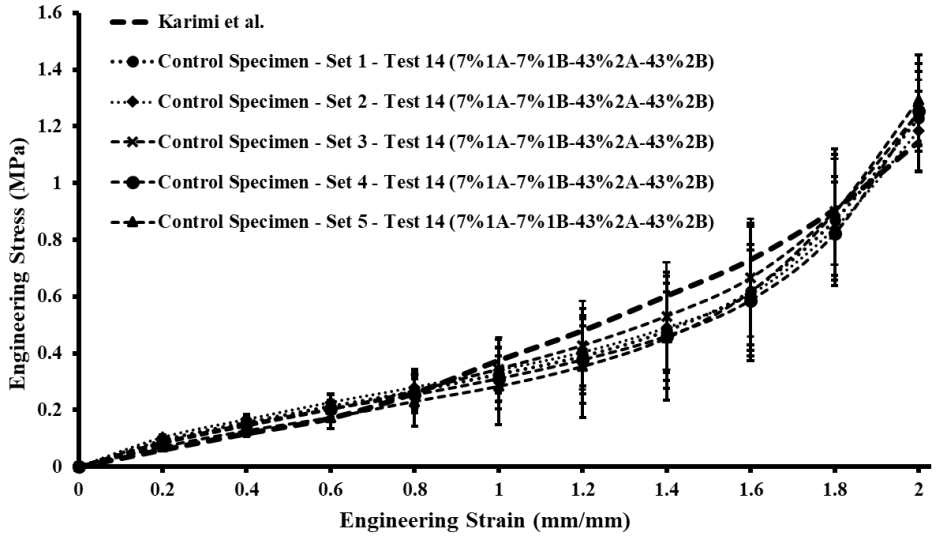


**Fig. 5.** Control specimen (mean ±S.D.) mimicking the mechanical behavior of liver tissue [13], tested for repeatability

### *3.3 Hyperelastic Curve Fitting of Liver Tissue Surrogates*

The non-linear hyperelastic characterization is commonly used to study the non-linear behavior of soft materials, such as elastomers and human soft tissues [15,27,28]. Eq. 7 was used to fit curves to the stress versus strain graphs obtained from the experimental testing. Table 2 summarizes the estimated values of $c_1$, $c_2$, *and* $c_3$ for the analyzed samples. All of the experimental tests showed an $R^2$ value of more than 0.97, and the Yeoh model showed an average $R^2$ value of 0.983, based on the recorded data.

**Table 2**
Coefficients of hyperelastic curve fit model for developed liver tissue simulants

| Experimental tests | Yeoh hyperelastic model coefficients | | |
|---|---|---|---|
| | $c_1$ | $c_2$ | $c_3$ |
| Test 1 | 0.00607 | 0.000004 | 0.0000119 |
| Test 2 | 0.01019 | 0.000006 | 0.0000291 |
| Test 3 | 0.00958 | 0.000011 | 0.0000604 |
| Test 4 | 0.01434 | 0.000014 | 0.0000378 |
| Test 5 | 0.01353 | 0.000017 | 0.0000471 |
| Test 6 | 0.01278 | 0.000019 | 0.0000515 |
| Test 7 | 0.01385 | 0.000023 | 0.0000565 |
| Test 8 | 0.01396 | 0.000026 | 0.0000657 |
| Test 9 | 0.02267 | 0.000028 | 0.0000854 |
| Test 10 | 0.02559 | 0.000031 | 0.0000907 |
| Test 11 | 0.02872 | 0.000037 | 0.0001250 |
| Test 12 | 0.03184 | 0.000040 | 0.0001403 |
| Test 13 | 0.04126 | 0.000043 | 0.0001417 |
| Test 14 | 0.04358 | 0.000059 | 0.0001988 |
| Test 15 | 0.04961 | 0.000065 | 0.0002115 |

## 4. Conclusions

In the reported work, a four-part elastomer material system was used to mimic the biomechanical behavior of human liver tissue. The fabricated test coupon samples for potential candidate of liver tissue surrogates were uniaxially tested under six different strain rates. A total of ninety experimental trials, consisting of fifteen coupons and six strain rates, with each test performed thrice to ensure precision. The mechanical behavior of the fabricated liver tissue samples was compared to existing literature on cadaveric tissue samples, and a non-linear hyperelastic curve fit model was used to predict the mechanical behavior of the fabricated tissue surrogates. The four-part elastomer-based material system has some limitations that should be considered for future work. Firstly, the used material system exhibited isotropic behavior and could not include anisotropic properties. Soft tissues exhibit isotropic and transversely isotropic properties when subjected to uniaxially tensile testing [15]. It was observed that there was no significant variation in the results at low strain rates (i.e., <1). However, for the cadaveric tissue samples, strain rates significantly affect the stress versus strain plots even at very low strains.

The fabricated liver tissue surrogates do not have any ethical or biosafety problems related to the experimental handling of cadaveric samples in laboratory settings. The use of such precisely developed tissue surrogates in the clinical setting would benefit surgical training, educational purposes, injury biomechanics, and the research of a wide variety of liver disorders, including liver cirrhosis, fatty liver, and liver fibrosis. Such tissue surrogates are also expected to be beneficial in investigating liver biomechanics and researching a variety of trauma scenarios.

## Author Contributions

Conceptualization, A.C.; methodology, G.S.; software, G.S.; validation, G.S.; formal analysis, G.S.; investigation, G.S.; data curation, G.S.; writing—original draft preparation, G.S.; writing—review and editing, G.S. and A.C.; supervision, A.C. All authors have read and agreed to the published version of the manuscript.

## Funding

This research received no external funding.

## Data Availability Statement

The data that support the findings of this study are available on request from the corresponding author.

## Conflicts of Interest

The authors declare that they have no known competing financial interests or personal relationships that could have appeared to influence the work reported in this paper.

## Acknowledgement

Gurpreet Singh is grateful to the Ministry of Education, Government of India, for awarding the Prime Minister's Research Fellowship (Ref: IITD/Admission/Ph.D./PMRF/2020-21/4062) for pursuing his doctoral research program at IIT-Delhi, India.

## References

[1] Welsh, R. H., Morris, A. P., & Hassan, A. M. (2007). Struck-side crashes involving post-regulatory European passenger cars: Crash characteristics and injury outcomes. International Journal of Vehicle Safety, 2(1–2), 103–115. https://doi.org/10.1504/IJVS.2007.012588

[2] Tinkoff, G., Esposito, T. J., Reed, J., Kilgo, P., Fildes, J., Pasquale, M., & Meredith, J. W. (2008). American Association for the Surgery of Trauma Organ Injury Scale I: Spleen, Liver, and Kidney, Validation Based on the National Trauma Data Bank. Journal of the American College of Surgeons, 207(5), 646–655. https://doi.org/10.1016/J.JAMCOLLSURG.2008.06.342

[3] Johnson, B., Campbell, S., & Campbell-Kyureghyan, N. (2021). Characterizing the Material Properties of the Kidney and Liver in Unconfined Compression and Probing Protocols with Special Reference to Varying Strain Rate. Biomechanics 2021, Vol. 1, Pages 264-280, 1(2), 264–280. https://doi.org/10.3390/BIOMECHANICS1020022

[4] Aycock, R. S., & Seyer, J. M. (1989). Collagens of Normal and Cirrhotic Human Liver. Connective Tissue Research, 23(1), 19–31. https://doi.org/10.3109/03008208909103901

[5] Yang, L., Fitié, C. F. C., van der Werf, K. O., Bennink, M. L., Dijkstra, P. J., & Feijen, J. (2008). Mechanical properties of single electrospun collagen type I fibers. Biomaterials, 29(8), 955–962. https://doi.org/10.1016/J.BIOMATERIALS.2007.10.058

[6] Nava, A., Mazza, E., Kleinermann, F., Avis, N. J., McClure, J., & Bajka, M. (2004). Evaluation of the mechanical properties of human liver and kidney through aspiration experiments. Technology and Health Care, 12(3), 269–280. https://doi.org/10.3233/THC-2004-12306

[7] Chatelin, S., Oudry, J., Périchon, N., Sandrin, L., Allemann, P., Soler, L., & Willinger, R. (2011). In vivo liver tissue mechanical properties by transient elastography: Comparison with dynamic mechanical analysis. Biorheology, 48(2), 75–88. https://doi.org/10.3233/BIR-2011-0584

[8] Yamashita, Y., & Kubota, M. (1995). Ultrasonic imaging of elasticity of soft tissue based on measurement of internal displacement and strain. Proceedings of the IEEE Ultrasonics Symposium, 2, 1207–1211. https://doi.org/10.1109/ULTSYM.1995.495777

[9] Sakuma, I., Nishimura, Y., Chui, C. K., Kobayashi, E., Inada, H., Chen, X., & Hisada, T. (2003). In vitro measurement of mechanical properties of liver tissue under compression and elongation using a new test piece holding method with surgical glue. Lecture Notes in Computer Science (Including Subseries Lecture Notes in Artificial Intelligence and Lecture Notes in Bioinformatics), 2673, 284–292. https://doi.org/10.1007/3-540-45015-7_27/COVER

[10] Ghadiali, S. N., Banks, J., & Swarts, J. D. (2004). Finite element analysis of active Eustachian tube function. Journal of Applied Physiology, 97(2), 648–654. https://doi.org/10.1152/JAPPLPHYSIOL.01250.2003/ASSET/IMAGES/LARGE/ZDG0080432320005.JPEG

[11] Wang, B. C., Wang, G. R., Yan, D. H., & Lid, Y. P. (1992). An Experimental Study on Biomechanical Properties of Hepatic Tissue Using a New Measuring Method. Bio-Medical Materials and Engineering, 2(3), 133–138. https://doi.org/10.3233/BME-1992-2305

[12] Stingl, J., Báča, V., Čech, P., Kovanda, J., Kovandová, H., Mandys, V., Rejmontová, J., & Sosna, B. (2002). Morphology and some biomechanical properties of human liver and spleen. Surgical and Radiologic Anatomy, 24(5), 285–289. https://doi.org/10.1007/S00276-002-0054-1/METRICS

[13] Karimi, A., & Shojaei, A. (2018). An Experimental Study to Measure the Mechanical Properties of the Human Liver. Digestive Diseases, 36(2), 150–155. https://doi.org/10.1159/000481344

[14] Loftis, K. L., Mazuchowski, E. L., Clouser, M. C., & Gillich, P. J. (2019). Prominent Injury Types in Vehicle Underbody Blast. Military Medicine, 184(Supplement_1), 261–264. https://doi.org/10.1093/MILMED/USY322

[15] Singh, G., & Chanda, A. (2021). Mechanical properties of whole-body soft human tissues : a review. Biomedical Materials, 16(6), 062004. https://doi.org/10.1088/1748-605X/ac2b7a

[16] Singh, G., Gupta, V., & Chanda, A. (2022b). Mechanical Characterization of Rotating Triangle Shaped Auxetic Skin Graft Simulants. Facta Universitatis, Series: Mechanical Engineering, 0(0), 1–16. https://doi.org/10.22190/FUME220226038S

[17] Makode, S., Singh, G., & Chanda, A. (2021). Development of novel anisotropic skin simulants. Physica Scripta, 96(12), 125019. https://doi.org/10.1088/1402-4896/AC2EFD

[18] Singh, G., Gupta, V., & Chanda, A. (2022a). Artificial skin with varying biomechanical properties. Materials Today: Proceedings, 62, 3162–3166. https://doi.org/10.1016/J.MATPR.2022.03.433

[19] Singh, G., & Chanda, A. (2023d). Development and biomechanical testing of artificial surrogates for vaginal tissue. Advances in Materials and Processing Technologies. https://doi.org/10.1080/2374068X.2023.2198837
[20] Bisplinghoff, J. A., Kemper, A. R., & Duma, S. M. (2012). Dynamic material properties of the pregnant human uterus. Journal of Biomechanics, 45(9), 1724–1727. https://doi.org/10.1016/J.JBIOMECH.2012.04.001
[21] Martins, Pedro A.L.S., Filho, A. L. S., Fonseca, A. M. R. M. I., Santos, A., Santos, L., Mascarenhas, T., Jorge, R. M. N., & Ferreira, A. J. M. (2011). Uniaxial mechanical behavior of the human female bladder. International Urogynecology Journal, 22(8), 991–995. https://doi.org/10.1007/s00192-011-1409-0
[22] Egorov, V. I., Schastlivtsev, I. V., Prut, E. V., Baranov, A. O., & Turusov, R. A. (2002). Mechanical properties of the human gastrointestinal tract. Journal of Biomechanics, 35(10), 1417–1425. https://doi.org/10.1016/S0021-9290(02)00084-2
[23] Bourgouin, S., Bège, T., Masson, C., Arnoux, P. J., Mancini, J., Garcia, S., Brunet, C., & Berdah, S. V. (2012). Biomechanical characterisation of fresh and cadaverous human small intestine: Applications for abdominal trauma. Medical and Biological Engineering and Computing, 50(12), 1279–1288. https://doi.org/10.1007/S11517-012-0964-Y/FIGURES/6
[24] Jin, X., Zhu, F., Mao, H., Shen, M., & Yang, K. H. (2013). A comprehensive experimental study on material properties of human brain tissue. Journal of Biomechanics, 46(16), 2795–2801. https://doi.org/10.1016/J.JBIOMECH.2013.09.001
[25] Kemper, A. R., Santago, A. C., Stitzel, J. D., Sparks, J. L., & Duma, S. M. (2012). Biomechanical response of human spleen in tensile loading. Journal of Biomechanics, 45(2), 348–355. https://doi.org/10.1016/j.jbiomech.2011.10.022
[26] Polio, S. R., Kundu, A. N., Dougan, C. E., Birch, N. P., Ezra Aurian-Blajeni, D., Schiffman, J. D., Crosby, A. J., & Peyton, S. R. (2018). Cross-platform mechanical characterization of lung tissue. PLOS ONE, 13(10), e0204765. https://doi.org/10.1371/JOURNAL.PONE.0204765
[27] Singh, G., & Chanda, A. (2023c). Biofidelic gallbladder tissue surrogates. Advances in Materials and Processing Technologies. https://doi.org/10.1080/2374068X.2023.2198835
[28] Singh, G., & Chanda, A. (2023e). Development and mechanical characterization of artificial surrogates for brain tissues. Biomedical Engineering Advances, 5, 100084. https://doi.org/10.1016/J.BEA.2023.100084
[29] Shergold, O. A., Fleck, N. A., & Radford, D. (2006). The uniaxial stress versus strain response of pig skin and silicone rubber at low and high strain rates. International Journal of Impact Engineering, 32(9), 1384–1402. https://doi.org/10.1016/J.IJIMPENG.2004.11.010
[30] Singh, G., & Chanda, A. (2023a). Biofidelic Tongue and Tonsils Tissue Surrogates. Materials Horizons: From Nature to Nanomaterials, Part F1471, 159–170. https://doi.org/10.1007/978-981-99-5064-5_10
[31] Singh, G., & Chanda, A. (2023b). Development and Biomechanical Testing of Human Stomach Tissue Surrogates. Materials Horizons: From Nature to Nanomaterials, Part F1471, 113–125. https://doi.org/10.1007/978-981-99-5064-5_7/TABLES/2
[32] Martins, P. A. L. S., Natal Jorge, R. M., & Ferreira, A. J. M. (2006). A Comparative Study of Several Material Models for Prediction of Hyperelastic Properties: Application to Silicone-Rubber and Soft Tissues. Strain, 42(3), 135–147. https://doi.org/10.1111/j.1475-1305.2006.00257.x
[33] Velardi, F., Fraternali, F., & Angelillo, M. (2006). Anisotropic constitutive equations and experimental tensile behavior of brain tissue. Biomechanics and Modeling in Mechanobiology, 5(1), 53–61. https://doi.org/10.1007/S10237-005-0007-9/METRICS
[34] Christ, A. F., Franze, K., Gautier, H., Moshayedi, P., Fawcett, J., Franklin, R. J. M., Karadottir, R. T., & Guck, J. (2010). Mechanical difference between white and gray matter in the rat cerebellum measured by scanning force microscopy. Journal of Biomechanics, 43(15), 2986–2992. https://doi.org/10.1016/J.JBIOMECH.2010.07.002